THE MULTISELECTIVITY SCHEME: A PYRAMIDAL ORGANIZATION OF WAVELETS WITH VARIABLE ANGULAR SELECTIVITY

J-P. Antoine and L. Jacques

Institut de Physique Théorique, Université Catholique de Louvain,
B - 1348 Louvain-la-Neuve, Belgium
email: antoine@fyma.ucl.ac.be, ljacques@fyma.ucl.ac.be
(Corresponding author: J-P. Antoine)

ABSTRACT

During the last ten years, many techniques have been devised to add directionality in image processing. We may cite, for instance, directional wavelets [1], steerable filters [8], curvelets [2], contourlets [5], ... This has opened the door to new ways for efficiently representing objects by oriented atoms. Real images, however, contain more than just smooth curves and straight lines defining contours of objects. They can present also details that are less oriented and more isotropic (like corners, spots, texture elements, ...). We present in this paper a tool which can be tuned relatively to these image features by decomposing them into a (linear) frame of directional wavelets with variable angular selectivity. To obtain such a decomposition, these new functions exploit some particularities of the (biorthogonal) circular multiresolution framework in the frequency domain. This link suggests the name of our method, 'multiselectivity analysis'.

1. INTRODUCTION

An image f of finite energy, that is, $f \in L^2(\mathbb{R}^2)$, can be analyzed by an admissible wavelet $\psi \in L^1(\mathbb{R}^2) \cap L^2(\mathbb{R}^2)$ through the continuous wavelet transform (CWT) [1] defined by

$$W_f(\vec{b},a,\theta) = \langle \psi_{\vec{b},a,\theta} | f \rangle \quad (1)$$

$$= \tfrac{1}{a^2} \int_{\mathbb{R}^2} \mathrm{d}^2\vec{x}\; \psi^*\big(a^{-1} r_\theta^{-1}(\vec{x}-\vec{b})\big)\, f(\vec{x}) \quad (2)$$

$$= \tfrac{1}{(2\pi)^2} \int_{\mathbb{R}^2} \mathrm{d}^2\vec{k}\; \widehat{\psi}^*(a r_\theta^{-1}\vec{k})\, \widehat{f}(\vec{k})\, e^{i\vec{k}\cdot\vec{b}}, \quad (3)$$

where * denotes the complex conjugation, $\psi_{\vec{b},a,\theta}$ is an L^1-normalized copy of ψ, translated by $\vec{b} \in \mathbb{R}^2$, dilated by $a \in \mathbb{R}_+$ and rotated by $\theta \in S^1 \simeq [0, 2\pi)$. In these equations, r_θ is the usual 2×2 rotation matrix, and the hat denotes the standard Fourier transform on $L^2(\mathbb{R}^2)$, that is, $\widehat{f}(\vec{k}) = \int_{\mathbb{R}^2} \mathrm{d}^2\vec{x}\; f(\vec{x})\; e^{-i\vec{k}\vec{x}}$, with inverse $f(\vec{x}) = (2\pi)^{-2} \int_{\mathbb{R}^2} \mathrm{d}^2\vec{k}\; \widehat{f}(\vec{k})\; e^{i\vec{k}\vec{x}}$.

Eq. (3) tells us that, if $\widehat{\psi}$ has a support mainly contained in a convex cone with apex on the origin, the wavelet ψ is able to detect locally oriented features in f for which frequencies are roughly located at the same place in the Fourier domain (e.g. straight lines). The angular selectivity of ψ, that is, its capacity to distinguish very close orientations, is also inversely proportional to the aperture of the supporting cone [1].

Suppose now the wavelet $\widehat{\psi}$ is separable in polar coordinate, that is,

$$\widehat{\psi}(\vec{k}) = \rho(k)\, \varphi(\kappa), \quad (4)$$

where $\vec{k} \equiv (k,\kappa)$, $k = |\vec{k}|$, $\kappa = \arg\vec{k}$ and φ is a positive function in $L^2(S^1, \mathrm{d}\kappa)$. The directionality of ψ is now controlled by the size of the support of φ.

In that case, the wavelet transform (1) becomes

$$W_f(\vec{b},a,\theta) = \langle \varphi_\theta | R_{\vec{b},a} \rangle_{S^1}, \quad (5)$$

where $\varphi_\theta(\kappa) = \varphi(\kappa - \theta)$, $\langle \cdot | \cdot \rangle_{S^1}$ is the scalar product of two functions on S^1, and $R_{\vec{b},a}$ is the angular function

$$R_{\vec{b},a}(\kappa) = \int_{\mathbb{R}_+} k\mathrm{d}k\; \rho^*(ak)\, \widehat{f}(k,\kappa)\, e^{ikb\cos(\kappa-\beta)}. \quad (6)$$

In other words, the coefficient W_f can be interpreted as the approximation of $R_{\vec{b},a}$ obtained by φ around the angle θ.

Let now D_ε be a dilation by a factor $\varepsilon \in \mathbb{R}_+$ on S^1 (its action may be obtained, for instance, by dilating a function of $L^2(\mathbb{R})$ and then periodizing it on S^1 [6]). We define the new coefficients

$$W_f(\vec{b},a,\varepsilon,\theta) = \langle \varphi_{\varepsilon,\theta} | R_{\vec{b},a} \rangle_{S^1}, \quad (7)$$

where $\varphi_{\varepsilon,\theta} = D_\varepsilon \varphi_\theta$, corresponding to the 2-D wavelet $\widehat{\psi}_\varepsilon(\vec{k}) = \rho(k)\varphi_{\varepsilon,0}(\kappa)$. This highly redundant construction is angularly very similar to the one obtained for the 1-D CWT [1]. In addition, the angular selectivity of ψ_ε is proportional to ε^{-1}. Thus we may expect that very oriented features in f will be well represented for small ε, while more isotropic ones will correspond to a bigger ε. This point will be made quantitative in Section 4 with the help of a (circular) biorthogonal multiresolution analysis, described in Section 3. We show in Section 5 how to adapt the angular selectivity of the wavelet to the content of an image. Finally, the method is illustrated on an example in Section 7.

2. DIRECTIONAL FRAMES OF WAVELETS

From the half-continuous frame theory [9], the continuous wavelet transform given in (1) can be discretized in its parameters a and θ while preserving a perfect reconstruction formula. Given a wavelet $\psi \in L^2(\mathbb{R}^1) \cap L^2(\mathbb{R}^2)$ with the polar separable form (4), we consider the dyadic discretization of scales $a_j = a_0 2^{-j}$ ($j \in \mathbb{Z}$, $a_0 \in \mathbb{R}_+$) and the regular discretization of angles $\theta_n = n\frac{2\pi}{N}$ ($n \in \mathbb{Z}[N] := \{0..N-1\}$, $N \in \mathbb{N}^0$). If the *frame property* is satisfied, that is, if there exist two constants $m, M \in \mathbb{R}_+^*$ such that,

$$m \leqslant \sum_{j\in\mathbb{Z}} \sum_{n\in\mathbb{Z}[N]} |\rho(a_j k)|^2\, |\varphi(\kappa - \theta_n)|^2 \leqslant M, \quad (8)$$

a.e. for $(k,\kappa) \in \mathbb{R}_+ \times S^1$, then $f \in L^2(\mathbb{R}^2)$ can be rebuilt as

$$f(\vec{x}) \;=\; \sum_{j\in\mathbb{Z}} \sum_{n\in\mathbb{Z}[N]} W_{j,n} \star \widetilde{\psi}_{a_j,\theta_n}(\vec{x}), \tag{9}$$

where $\widetilde{\psi}$ is a certain dual wavelet, and with $W_{j,n}(\vec{b}) = W_f(\vec{b}, a_j, \theta_n)$.

A particular case is obtained when

$$\sum_{j\in\mathbb{Z}} \sum_{n\in\mathbb{Z}[N]} \rho(a_j k)\, \varphi(\kappa - \theta_n) \;=\; A, \quad A \in \mathbb{R}_+^*, \tag{10}$$

a.e. for $(k,\kappa) \in \mathbb{R}_+ \times S^1$. This defines a *linear frame*, for which $\widetilde{\psi} = \delta$, so that we have the *Littlewood-Paley* decomposition

$$f(\vec{x}) \;=\; A^{-1} \sum_{j\in\mathbb{Z}} \sum_{n\in\mathbb{Z}[N]} W_{j,n}(\vec{x}). \tag{11}$$

Finally, both in the general case and in the linear case, a scaling function can be introduced to fix a lower bound to the available resolutions j. For a linear frame, we define the function

$$\widehat{\zeta}(\vec{k}) = \sum_{j=-\mathbb{N}} \sum_{n\in\mathbb{Z}[N]} \widehat{\psi}(a_j r_{\theta_n}^{-1} \vec{k}). \tag{12}$$

Thus, writing $S_j(\vec{b}) = \langle \zeta_{\vec{b},j} | f \rangle$, we have, for $J \in \mathbb{N}$,

$$f(\vec{x}) \;=\; A^{-1} S_{-J}(\vec{x}) + A^{-1} \sum_{j=-J+1}^{\infty} \sum_{n\in\mathbb{Z}[N]} .W_{j,n}(\vec{x}). \tag{13}$$

3. BIORTHOGONAL MULTIRESOLUTION ON C^1

Consider a biorthogonal multiresolution analysis in $L^2(\mathbb{R})$ [4] generated by a scaling function $\phi \in L^2(\mathbb{R})$ and a wavelet $\chi \in L^2(\mathbb{R})$, both biorthogonal to their dual counterparts $\widetilde{\phi}, \widetilde{\chi} \in L^2(\mathbb{R})$. All these functions are linked through their *refinement equations* to the filters h, g, $\widetilde{h}$ and $\widetilde{g}$. For instance,

$$\frac{1}{\sqrt{2}}\, \phi\Big(\frac{t}{2}\Big) \;=\; \sum_{n\in\mathbb{Z}} h[n]\, \phi(t-n). \tag{14}$$

This multiresolution analysis can be adapted on the circle $C^1 \simeq [0,1)$ [4]. Writing $u_{l,n}(t) = 2^{l/2} u(2^l t - n)$ for any function $u \in L^2(\mathbb{R})$, we define the periodized version of $\phi_{l,n}$ as

$$\Phi_{l,n}(t) \;=\; \sum_{m\in\mathbb{Z}} \phi_{l,n}(t+m), \quad t \in C^1. \tag{15}$$

The same operation applied on $\chi_{l,n}$, $\widetilde{\phi}_{l,n}$ and $\widetilde{\chi}_{l,n}$ leads, respectively, to $\chi_{l,n}$, $\widetilde{\Phi}_{l,n}$ and $\widetilde{\chi}_{l,n} \in L^2(C^1)$.

Since, for $l \geqslant 0$, $\mathbf{u}_{l,n}(t) = \mathbf{u}_{l,n+2^l r}(t)$ for any function $\mathbf{u}_{l,n}$ obtained by a periodization of a function $u_{l,n} \in L^2(\mathbb{R})$, the spaces $\mathbf{V}_l = \{\Phi_{l,n} : n \in \mathbb{Z}[2^l]\}$, $\mathbf{W}_l = \{\chi_{l,n} : n \in \mathbb{Z}[2^l]\}$ and their dual equivalents have all the same finite dimension 2^l.

If we require that ϕ and $\widetilde{\phi}$ realize a partition of unity, that is, if $\sum_{m\in\mathbb{Z}} \phi(t-m) = \sum_{m\in\mathbb{Z}} \widetilde{\phi}(t-m) = 1$, it can be proved [4] that, for all $t \in \mathbb{R}$, $\Phi_{l,n}(t) = \widetilde{\Phi}_{l,n}(t) = 2^{-l/2}$ for $l \leqslant 0$, and $\chi_{l,n}(t) = \widetilde{\chi}_{l,n}(t) = 0$ for $l < 0$. As a consequence, for all $l \leqslant 0$, $\mathbf{V}_l$ and $\widetilde{\mathbf{V}}_l$ consist of constant functions on C^1, while for all $l < 0$, $\mathbf{W}_l$ and $\widetilde{\mathbf{W}}_l$ reduce to the zero function.

In addition, $\mathbf{V}_l$ and $\widetilde{\mathbf{W}}_l$, and also $\widetilde{\mathbf{V}}_l$ and $\mathbf{W}_l$, are still orthogonal since, $\forall l, l' \in \mathbb{N}$, $\forall n \in \mathbb{Z}[2^l]$, and $\forall n' \in \mathbb{Z}[2^{l'}]$,

$$\langle \mathbf{u}_{l,n} | \mathbf{v}_{l',n'} \rangle_{C^1} \;=\; \sum_{q\in\mathbb{Z}} \langle u_{l,n} | v_{l,n'-2^{l'}q} \rangle, \tag{16}$$

for the functions $\mathbf{u}_{l,n}$ and $\mathbf{v}_{l,n}$ obtained by periodization of two functions $u_{l,n}$ and $v_{l,n}$, and with the scalar product $\langle \cdot | \cdot \rangle_{C^1}$ taken on C^1.

In conclusion, since the inclusions $\mathbf{V}_l \subset \mathbf{V}_{l+1}$, $\mathbf{W}_l \subset \mathbf{W}_{l+1}$, $\widetilde{\mathbf{V}}_l \subset \widetilde{\mathbf{V}}_{l+1}$, and $\widetilde{\mathbf{W}}_l \subset \widetilde{\mathbf{W}}_{l+1}$ are inherited from $\mathbb{R}$, we obtain a biorthogonal multiresolution analysis on C^1 generated by the functions $\Phi_{l,n}$, $\chi_{l,n}$, $\widetilde{\Phi}_{l,n}$, and $\widetilde{\chi}_{l,n}$.

Writing $s_l[n] = \sum_{m\in\mathbb{Z}} s[n + 2^l m]$ for a sequence $s \in l^2(\mathbb{Z})$, these four functions are linked to the filters $h_l[n]$, $g_l[n]$, $\widetilde{h}_l[n]$ and $\widetilde{g}_l[n]$ through the refinement equations

$$\Phi_{l-1,n}(t) = \sum_{q\in\mathbb{Z}[2^l]} h_l[q-2n]\, \Phi_{l,q}(t), \tag{17}$$

$$\chi_{l-1,n}(t) = \sum_{q\in\mathbb{Z}[2^l]} g_l[q-2n]\, \Phi_{l,q}(t), \tag{18}$$

and similarly for the dual counterparts.

In addition, a reconstruction from resolution l to resolution $l+1$ is possible with

$$\begin{aligned} \Phi_{l+1,n}(t) \;=\; & \sum_{m\in\mathbb{Z}[2^l]} \widetilde{h}_{l+1}[n-2m]\, \Phi_{l,m}(t) \\ & + \sum_{m\in\mathbb{Z}[2^l]} \widetilde{g}_{l+1}[n-2m]\, \chi_{l,m}(t). \end{aligned} \tag{19}$$

4. MULTISELECTIVITY ANALYSIS

From the circular biorthogonal multiresolution analysis detailed in the previous section, we create 2-D directional wavelets with the following properties:

- They combine with each other in a pyramidal scheme to form wavelets with a lower angular selectivity until one obtains a totally isotropic one;
- They define a half-continuous linear frame for each *selectivity level*.

With the notations of the previous section, we first define the new wavelets

$$\widehat{\psi}^{\mathrm{a}}_{l,n}(\vec{k}) = \rho(k)\, \varphi_{l,n}(\kappa), \tag{20}$$

$$\widehat{\psi}^{\mathrm{d}}_{l,n}(\vec{k}) = \rho(k)\, \gamma_{l,n}(\kappa), \tag{21}$$

with $\vec{k} = (k,\kappa)$ in polar coordinates, $\varphi_{l,n}(\kappa) = \phi_{l,n}(\frac{\kappa}{2\pi})$ and $\gamma_{l,n}(\kappa) = \chi_{l,n}\big(\frac{\kappa}{2\pi}\big)$, the analogues of ϕ and χ on the circle $S^1 \simeq [0, 2\pi)$. The exponents a and d labeling the two wavelets remind that they are related to *approximation* and *detail* functions in the multiresolution scheme.

Notice that the parameter n stands for a rotation, since $\widehat{\psi}^{\mathrm{a}}_{l,n}(\vec{k}) = \widehat{\psi}^{\mathrm{a}}_{l,0}(r_{\theta_n}^{-1}\vec{k})$, while the parameter l determine a *selectivity level*. Indeed, the half-aperture $\alpha \in [0,\pi]$ of the cone supporting $\widehat{\psi}^{\mathrm{a}}_{l,n}$ and $\widehat{\psi}^{\mathrm{d}}_{l,n}$ is proportional to 2^{-l}, which means that the angular selectivity of these wavelets growths with l [7]. This behavior is shown in Figure 1 for the wavelets described in Section 6 below. In this particular case, we have $\alpha = 2^{-l+2}\pi$ for $l \geqslant 2$, so that the wavelet $\widehat{\psi}^{\mathrm{a,d}}_{l,n}$ is conical for $l \geqslant 4$ [1].

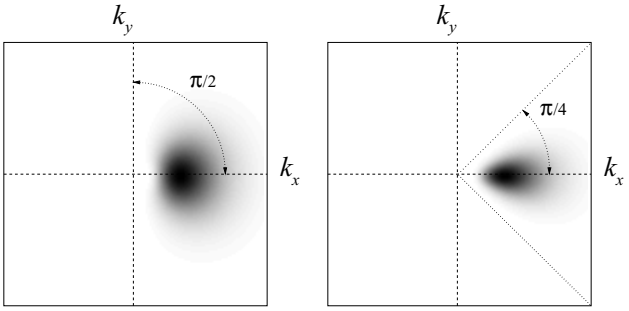

Figure 1: $\widehat{\psi}^{\mathrm{a}}_{3,0}(\vec{k})$, with $\alpha=\pi/2$ (left); $\widehat{\psi}^{\mathrm{a}}_{4,0}(\vec{k})$ with $\alpha=\pi/4$; this is a conical wavelet (right).

Proposition 1 *Let $a_j = a_0 2^{-j}$ be a dyadic scale discretization. If $\sum_{j\in\mathbb{Z}} \rho(a_j k) = 1$ a.e. for $k \in \mathbb{R}_+$, then, for any $l \in \mathbb{N}$, the family $\{\psi^{\mathrm{a}}_{j,l,n} : j \in \mathbb{Z}, n \in \mathbb{Z}[2^l]\}$ is a linear frame of $L^2(\mathbb{R}^2)$, i.e., it obeys* (10) *with $A = 2^{l/2}c$.*

A proof may be found in [7]. Hence, given a function $f \in L^2(\mathbb{R}^2)$, we have, for $J \in \mathbb{N}$ and a fixed selectivity level $l \in \mathbb{N}$, the reconstruction formula (we put $c = 1$)

$$f(\vec{x}) \;=\; S_{-J}(\vec{x}) \;+\; \sum_{j=-J+1}^{\infty} \sum_{n\in\mathbb{Z}[2^l]} 2^{-l/2}\, W^{\mathrm{a}}_{j,l,n}(\vec{x}), \qquad (22)$$

with $W^{\mathrm{a}}_{j,l,n}(\vec{b}) \equiv \langle \psi^{\mathrm{a}}_{\vec{b},j,l,n} | f\rangle = \langle \varphi_{l,n} | R_{\vec{b},a_j} \rangle_{S^1}$, and the 2-D scaling function $\hat{\zeta}(\vec{k}) = \sum_{j\in-\mathbb{N}} \rho(a_j k)$.

Notice that, from the recursion rules (17) and (18),

$$\begin{aligned} W^{\mathrm{a}}_{j,l-1,n}(\vec{b}) &= \sum_{n'\in\mathbb{Z}[2^l]} h^*_l[n'-2n]\, W^{\mathrm{a}}_{j,l,n'}(\vec{b}) \\ &= \big(\bar{h}_l \circledast W^{\mathrm{a}}_{j,l,\cdot}(\vec{b})\big)_{2n}, \qquad (23) \\ W^{\mathrm{d}}_{j,l-1,n}(\vec{b}) &= \big(\bar{g}_l \circledast W^{\mathrm{a}}_{j,l,\cdot}(\vec{b})\big)_{2n}, \qquad (24) \end{aligned}$$

where $\bar{s}_l[n] = s^*_l[-n]$, $\circledast$ is the circular convolution between two sequences with the same period, and $(\cdot)_p$ means that we take the p^{th} orientation of the result. A reconstruction is also possible starting from (19), namely,

$$W^{\mathrm{a}}_{j,l+1,n}(\vec{b}) = \big(\breve{h}^*_{l+1} \circledast \breve{W}^{\mathrm{a}}_{j,l,\cdot}(\vec{b})\big)_n + \big(\breve{g}^*_{l+1} \circledast \breve{W}^{\mathrm{d}}_{j,l,\cdot}(\vec{b})\big)_n, \quad (25)$$

where $\breve{\cdot}$ is the oversampling operator defined by $\breve{s}[2n] = s[n]$ and $\breve{s}[2n+1] = 0$ for any sequence $s[n]$, acting here on the orientation parameter of the wavelet coefficients.

Equations (23), (24) and (25) tell us that the wavelet coefficients $W^{\mathrm{a,d}}_{j,l,n}(\vec{b})$ follow a pyramidal construction scheme with respect to the selectivity level l.

5. ADAPTIVE SELECTIVITY

With the linear frame described above, the selectivity level l can be adapted to the content of f.

Proposition 2 *Given a function $\widetilde{l} : \mathbb{R}^2 \times \mathbb{Z} \to \mathbb{N}$, $(\vec{x}, j) \mapsto \widetilde{l}(\vec{x}, j)$, and any index $J \in \mathbb{N}$, an element $f \in L^2(\mathbb{R}^2)$ can be decomposed as*

$$f(\vec{x}) \;=\; S_{-J}(\vec{x}) \;+\; \sum_{j=-J+1}^{\infty} \sum_{n\in\mathbb{Z}[2^{\widetilde{l}}]} 2^{-\widetilde{l}/2}\, W^{\mathrm{a}}_{j,\widetilde{l},n}(\vec{x}), \qquad (26)$$

This is a simple consequence of the identity $\sum_{n\in\mathbb{Z}[2^l]} 2^{-l/2} W^{\mathrm{a}}_{j,l,n}(\vec{x}) = W^{\mathrm{i}}_j(\vec{x})$, where $W^{\mathrm{i}}_j(\vec{x}) = W^{\mathrm{a}}_{j,0,0}(\vec{x})$ are the coefficients corresponding to the isotropic wavelet $\widehat{\psi}^{\mathrm{i}}(\vec{k}) = \rho(k)$.

Given a highest selectivity level $L \in \mathbb{N}$, $\widetilde{l}$ will be defined in the sequel as the level which yields the best match between the function f and a wavelet of this level, that is

$$\widetilde{l}(\vec{b}, j) \;=\; \operatorname*{arg\,max}_{l\in[0,L]} \max_{n\in\mathbb{Z}[2^l]} |\langle \psi^{\mathrm{a}}_{\vec{b},j,l,n} | f\rangle|\; a_j \|\psi^{\mathrm{a}}_{l,n}\|^{-1}. \qquad (27)$$

6. CHOICE OF THE WAVELETS

n	$h[n]$	$\widetilde{h}[n]$
$0,1$	0.53033008588991	0.95164212189718
$-1,2$	0.17677669529664	−0.02649924094535
$-2,3$		−0.30115912592284
$-3,4$		0.03133297870736
$-4,5$		0.07466398507402
$-5,6$		−0.01683176542131
$-6,7$		−0.00906325830378
$-7,8$		0.00302108610126

Table 1: CDF filters with $p = 3$ and $\widetilde{p} = 7$ vanishing moments.

For defining the functions ϕ and χ, thus their periodized versions ϕ and χ, we use the results of Cohen-Daubechies-Feauveau [3] on the construction of a compactly supported biorthogonal basis of wavelets with a given number of vanishing moments. In particular, we select the filters h and $\widetilde{h}$ with $p = 3$ and $\widetilde{p} = 7$ moments, respectively (see Table 1). This basis is linked to a quadratic B-spline (of order $p-1$) [10], and it guarantees a second order regularity on the edges of the cone supporting $\widehat{\psi}^{\mathrm{a,d}}_{l,n}(\vec{k})$.

Since Proposition 1 requires that $\sum_{j\in\mathbb{Z}} \rho(a_j k) = 1$, we choose simply $\rho(k) = \phi(\log_2 k)$, noting that the B-spline ϕ yields a partition of unity, i.e., $\sum_{m\in\mathbb{Z}} \phi(t+m) = 1$.

Numerically, all the analyzed functions f are discretized, and thus they are assumed to belong to $\mathscr{B}_\pi = \{f \in L^2(\mathbb{R}^2) : \widehat{f}(\vec{k}) = 0, \text{if } \|\vec{k}\|_\infty > \pi\}$. Since $\operatorname{supp}\phi = [-3/2, 3/2]$, by choosing $a_0 = 2^{3/2}\pi^{-1} \simeq 0.9003$ in the discretization of scale, $\operatorname{supp}\rho(a_0 k) \subset [\pi/8, \pi]$ and j must take negative values. So, up to certain high frequency residual functions [7], the reconstruction (13) remains valid for $j \in [-J+1, 0]$, with $J \in \mathbb{N}$ resolutions.

For every $l \in \mathbb{N}$, the linear frame $\{\psi^{\mathrm{a}}_{j,l,n}\}$ obtained with such a choice will be called the *Angular Spline Frame* (ASF) of fixed selectivity l. If the selectivity level is choosed adaptively according to the content of f, i.e., if $l = \widetilde{l}(\vec{x}, j)$, we will speak of an *adaptive* ASF.

7. NONLINEAR APPROXIMATIONS

For a frame $\mathscr{F} = \{\psi_\lambda \in L^2(\mathbb{R}^2)\}$, where λ stands for the parameters of the wavelets, we define the N-term nonlinear approximation of a function $f \in L^2(\mathbb{R}^2)$ by

$$f_N \;=\; \sum_{k=1}^{N} \langle \psi_{\lambda_k} | f\rangle\; \widetilde{\psi}_{\lambda_k}, \qquad (28)$$

where $\widetilde{\mathscr{F}} = \{\widetilde{\psi}_\lambda \in L^2(\mathbb{R}^2)\}$ is the dual frame of $\mathscr{F}$, and where λ_k is a reordering of the parameters λ s.t. $m_{\lambda_k} \equiv \|\psi_{\lambda_k}\|^{-1} |\langle \psi_{\lambda_k} | f \rangle| \geqslant m_{\lambda_{k+1}}$, $\forall k \in \mathbb{N}$. The value m_λ is called the *magnitude* of the coefficient $\langle \psi_\lambda | f \rangle$.

Unlike the case of the orthogonal bases, it is not guaranteed for frames that f_N is the best N-term nonlinear approximation. We will assume, however, that the error $\epsilon_f[N] = \|f - f_N\|$ is globally decreasing with N.

In this paper, we use nonlinear approximations to compare the fixed and the adaptive ASF methods.[1] However, these two frames do not have the same number of elements. Therefore, we define the τ%-term nonlinear approximation (with $\tau \in [0, 100]$) as the approximation obtained with $N = \lfloor \frac{\tau}{100} M \rfloor$ of the best terms, where M represents the total number of elements in the frame.

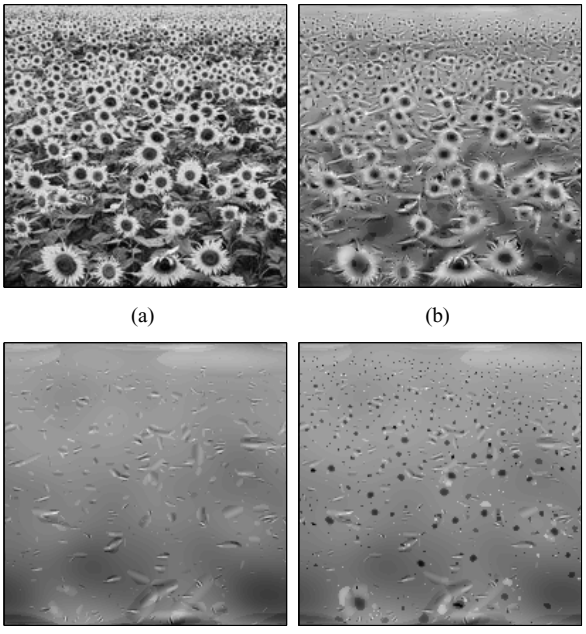

(a) (b) (c) (d)

Figure 2: τ%-term nonlinear approximations. (a) Original image (sunflower fields). (b) Adaptive ASF, 10%-term approximation (18.22 dB). (c) and (d) 1%-term approximation respectively for fixed (13.84 dB) and adaptive ASF (14.27 dB).

For comparing the fixed and the adaptive ASF methods, we analyze the image of a sunflower field (Fig. 2(a)). This picture presents both directional objects, like the sticks and the leaves of the plants, and more isotropic features like the dark center of the flowers. In addition, because of the angle of view of the camera, these elements appear at various scales, depending on their distance to the objective.

Figures 2(c) and 2(d) show nonlinear approximations obtained for 1% of the total number of terms in the fixed and adaptive methods, respectively. In each case, we take $L = 4$ (16 orientations) with $J = 5$ number of scales. The corresponding qualities of the approximations, expressed in PSNR, are equal to 13.84 dB and 14.27 dB. We can observe that, without losing the main directional objects, the adaptive method displays most of the dark centers of the flowers, whereas they are completely absent in the fixed selectivity method. This effect can be tested at higher percentages. For instance, for 10%-term approximations, the fixed ASF gives a PSNR of 16.72 dB, while the adaptive one provides a quality of 18.22 dB (Fig. 2(b)). This phenomenon is explained by the number of coefficients needed to render an object. To give an example, if a feature corresponds to a selectivity level $L-1$, the adaptive ASF saves $2^{L-1}-1$ coefficients, which are then used to described other features.

[1] In practice, we can "count" the positions $\vec{b}$, since they are discretized for a band limited function $f \in \mathscr{B}_\pi$

8. CONCLUSION

We have presented a new family of wavelets characterized by their controlled angular selectivity (through their selectivity level), and inheriting several multiresolution properties like the recursion rules, the linearity of the frame, and the directionality thanks to the compacity of the filters. Finally, in the context of nonlinear approximations obtained with a restricted number of terms, the last section has shown that the adaptive ASF method saves a certain number of coefficents which can then be reallocated to other features.

REFERENCES

[1] J-P. Antoine, R. Murenzi, P. Vandergheynst, and S. T. Ali. *Two-dimensional Wavelets and Their Relatives*. Cambridge University Press, Cambridge (UK), 2004. (in press).

[2] E. Candès and D. Donoho. Curvelets: A surprisingly effective nonadaptive representation for objects with edges. In *Curve and Surface Fitting*, Nashville, TN, 1999. Eds. L. L. Schumaker et al., Vanderbilt University.

[3] A. Cohen, I. Daubechies, and J. Feauveau. Biorthogonal bases of compactly supported wavelets. *Commun. Pure Appl. Math.*, **45**:485–560, 1992.

[4] I. Daubechies. *Ten Lectures on Wavelets*. SIAM, Philadelphia, PA, 1992.

[5] M.N. Do and M. Vetterli. Contourlets: A directional multiresolution image representation. In *Proc. IEEE Intern.Conf. on Image Processing*, **1**, pp. 357–360, Rochester, September 2002.

[6] M. Holschneider. Wavelet analysis on the circle. *J. Math. Phys.*, **31**:39–44, 1990.

[7] L. Jacques. *Ondelettes, repères et couronne solaire*. Thèse de doctorat, Université catholique de Louvain, Louvain-la-Neuve, Belgique, 2004. (to appear).

[8] A. Karasaridis and E. Simoncelli. A filter design technique for steerable pyramid image transforms. In *Intern. Conf. on Acoustics, Speech and Signal Processing*, Atlanta GA, May 1996.

[9] B. Torrésani. *Analyse continue par ondelettes*. InterÉditions/CNRS Éditions, Paris, 1995.

[10] M. Unser, A. Aldroubi, and M. Eden. B-Spline signal processing: Part I—Theory. *IEEE Trans. Signal Processing*, **41**(2):821–833, 1993.